

CRYSTALLIZATION AND THERMAL EXPANSION CHARACTERISTICS OF In_2O_3 -CONTAINING LITHIUM IRON SILICATE-DIOPSIDE GLASSES

S.M. SALMAN, S.N. SALAMA

Glass Research Dept., National Research Centre, El-Behoos St., Dokki, Cairo, Egypt

E-mail: s.moghazy@yahoo.com

Submitted October 13, 2010; accepted May 1, 2011

Keywords: In_2O_3 -containing glass, Crystallization, Thermal expansion

The crystallization characteristics of glasses based on lithium iron silicate ($\text{LiFeSi}_2\text{O}_6$)-diopside ($\text{CaMgSi}_2\text{O}_6$) composition with addition of Al_2O_3 at the expense of Fe_2O_3 were described. The effect of $\text{LiInSi}_2\text{O}_6/\text{CaMgSi}_2\text{O}_6$ replacements was also investigated. The thermal treatment, the crystal phases, and the micro-structural properties of ($\text{LiFeSi}_2\text{O}_6$ - $\text{CaMgSi}_2\text{O}_6$) glasses, replacing partial Fe_2O_3 with Al_2O_3 and partial $\text{CaMgSi}_2\text{O}_6$ with $\text{LiInSi}_2\text{O}_6$, have been studied by a differential thermal analysis, an X-ray diffraction, and a scanning electron microscopy. The glasses show the intense uniform bulk-crystallization with the fine grained microstructure by increasing the replacement of $\text{Al}_2\text{O}_3/\text{Fe}_2\text{O}_3$ and $\text{LiInSi}_2\text{O}_6/\text{CaMgSi}_2\text{O}_6$. The crystallizing phases of $\text{Ca}(\text{Fe,Mg})(\text{SiO}_3)_2$, α - LiFe_3O_8 , Li_2SiO_3 , α - SiO_2 and $\text{CaMgSi}_2\text{O}_6$ are mostly formed together; in most case, with $\text{Li}_{0.6}\text{Al}_{0.6}\text{Si}_{2.4}\text{O}_6$, β -eucryptite solid solution, $\text{LiInSi}_2\text{O}_6$, $\text{In}_2\text{Si}_2\text{O}_7$, and $\text{LiFeSi}_2\text{O}_6$. The Al_2O_3 partial replacement increases the transformation temperature (T_c) and softening one (T_s) for the glasses and the glass-ceramics, and decreases the thermal expansion coefficient (α -value) for the glasses. The $\text{LiInSi}_2\text{O}_6$ partial replacement decreases T_c and T_s and increases the α -value for the glasses, while the Al_2O_3 and $\text{LiInSi}_2\text{O}_6$ partial replacements decrease the α -value for the glass-ceramics. The crystallization characters of the glasses are correlated to the internal structure, as well as role played by the glass-forming cations. However, the one of the glass-ceramics are mainly attributed to the crystalline phases formed in the material.

INTRODUCTION

Glass-ceramics are a class of materials that are highly crystalline, have near-zero porosity. They thus represent the most precise and reliable ceramics produced today and are found in many important applications for which neither glass nor conventional ceramics are suitable [1].

An important feature of the glass-ceramic is that it is applicable to a wide range of compositions. The properties of glass-ceramics depend upon both composition and microstructure. Composition can be divided into two parts: bulk chemical composition and phase assemblage. The bulk chemical composition controls glass formation and workability, as well as the tendency toward internal nucleation and crystallization in general. The type and proportion of the crystalline and amorphous phases, controls the physical properties of the glass-ceramics [2].

Lithium aluminosilicates (LAS) glass ceramics attract considerable commercial interest because they mainly feature low expansion, together with remarkable chemical resistance and mechanical strength. LAS glass-ceramics with superior thermal properties are based on crystals of lithium aluminosilicates solid solution (high-

quartz, keatite, β -eucryptite, β -spodumene), and used at precision parts of optical observation systems, cooktop panels, stove windows, fire doors, cookware, and other technical devices [3,4].

The system $\text{CaO-MgO-Al}_2\text{O}_3\text{-SiO}_2$ is one of the best understood quaternary system in the non-metallic field, because of its application of materials based on this system, it attracted the attention and had been studied by many workers. Many different mineral phases and assemblages had shown to be associated with the course of crystallization of this system. It has been considered worthwhile to give a concise on some of the most important crystalline phases such as pyroxene and melilites[5].

Iron-rich glasses and glass-ceramics somewhat similar to natural basalt, were developed for nuclear waste disposal, because during vitrification the radioactive nuclides are incorporated in the chemically stable glass network [6].

The crystallization of semiconductive oxides has only been reported for TiO_2 , SnO_2 and In_2O_3 [7]. The latter is of special potential because of the large solubility of In_2O_3 in convenient silicate and borate melts. In_2O_3 is a large band gap n-type semiconductor. At the moment,

indium oxide is predominantly used as coating material for transparent electric conductors (e.g. as electrode material in OLED-devices) or, however, as infrared reflective material. Whereas glassy substrates can easily be coated by In_2O_3 using sputtering or sol-gel techniques [8].

The structure of multicomponent silicate glasses is based on a polymeric network with coexisting cations, which may act as modifiers or as charge compensating cations needed for balancing the charge deficit of oxygen neighbours. This situation occurs when trivalent cations are substituted to silicon in the polymeric network. Glass properties may be strongly affected, depending on whether cations are network modifiers or charge compensators. This has been shown in alkali-bearing glasses in which transport properties are strongly affected by the substitution of silicon by aluminium, in correlation with important structural modifications [9, 10].

The purpose of this work is to study the crystallization behaviour, phase relation, microstructure and the thermal expansion property of some multicomponent silicate glasses-containing In_2O_3 .

EXPERIMENTAL

Batch composition and glass preparation

The glass compositions were calculated to give different proportions of stoichiometric lithium iron silicate- $[\text{LiFeSi}_2\text{O}_6]$ - diopside $[\text{CaMgSi}_2\text{O}_6]$, with partial

replacements of Al_2O_3 and lithium indium silicate- $[\text{LiInSi}_2\text{O}_6]$ instead of Fe_2O_3 and diopside $[\text{CaMgSi}_2\text{O}_6]$, respectively. Details of the glass oxide constituents are given in Table 1.

Reagent grade powders of Li_2CO_3 , CaCO_3 , SiO_2 (quartz), MgCO_3 , $\text{Al}(\text{OH})_3$, In_2O_3 and Fe_2O_3 , forming the glass batches were melted in Pt-2%Rh-crucible in an electric furnace with SiC heating elements at 1350-1450 °C for 4 hrs. Melting was continued until a clear homogeneous melt was obtained; this was achieved by swirling the melt several times at about 30 min intervals. The melt was cast into rods and as buttons, which were then properly annealed in a muffle furnace at 650°C for 1 h then cooled at 1°C/min to room temperature to minimize the strain.

Differential thermal analysis

The thermal behaviour of the finely powdered (45-75 μm) glass samples was examined using a SETARAM LabSysTM TG-DSC16 under Ar gas atmosphere (at constant rate of 50°C/min). About 50 mg of the powdered glass was heated in Pt-holder with another Pt-holder containing Al_2O_3 as a reference material. A uniform heating rate of 10°C/min was adopted. Data were recorded using a computer-driven data acquisition system. The results obtained were used as a guide for determining the required heat-treatment temperatures applied to induce crystallization of the glasses.

Table 1. Composition of the studied glasses (wt.%).

Glass No.	$\text{LiFeSi}_2\text{O}_6$	$\text{CaMgSi}_2\text{O}_6$	$\text{LiInSi}_2\text{O}_6$	Li_2O	Fe_2O_3	CaO	MgO	SiO_2	In_2O_3	$\text{Al}_2\text{O}_3/\text{Fe}_2\text{O}_3$
G ₁	50	50	–	7.18	7.18	14.22	14.24	57.18	–	– mole %
	50	50	–	3.48	18.58	12.9	9.3	55.7	–	– wt. %
G ₂	50	50	–	7.18	3.18	14.22	14.24	57.18	–	4 mole %
	50	50	–	3.62	8.55	13.43	9.67	57.86	–	6.87 wt.%
G ₃	50	50	–	7.18	–	14.22	14.24	57.18	–	7.18 mole %
	50	50	–	3.73	–	13.86	9.98	59.71	–	12.72 wt.%
G ₄	50	40	10	8.60	7.44	11.81	11.82	58.03	2.3	– mole %
	50	40	10	4.02	18.58	10.36	7.45	54.53	5.068	– wt. %
G ₅	50	40	10	8.60	3.44	11.81	11.82	58.03	2.3	4 mole %
	50	40	10	4.17	8.92	10.75	7.74	56.62	5.18	6.62 wt. %
G ₆	50	40	10	4.02	–	11.81	11.82	58.03	2.3	7.44 mole%
	50	40	10	4.31	–	11.11	7.99	58.50	5.36	12.73 wt. %
G ₇	50	20	30	11.79	8.02	6.37	6.36	59.91	7.55	– mole%
	50	20	30	5.11	18.58	5.18	3.72	52.21	15.2	– wt. %
G ₈	50	20	30	11.79	4.02	6.37	6.36	59.91	7.55	4 mole %
	50	20	30	5.29	9.63	5.36	3.85	54.02	15.73	6.12 wt. %
G ₉	50	20	30	11.79	–	6.37	6.36	59.91	7.55	8.02 mole%
	50	20	30	5.48	–	5.55	3.98	55.97	16.30	12.72 wt. %
G ₁₀	50	–	50	15.52	8.71	–	–	62.11	13.66	– mole %
	50	–	50	6.20	18.58	–	–	49.88	25.34	– wt. %
G ₁₁	50	–	50	15.52	4.71	–	–	62.11	13.66	4 mole %
	50	–	50	6.39	10.37	–	–	51.47	26.15	5.62 wt. %
G ₁₂	50	–	50	15.52	–	–	–	62.11	13.66	8.71 mole %
	50	–	50	6.64	–	–	–	53.47	27.17	12.72 wt. %

The progress of crystallization in the glasses was followed using double stage heat-treatment regimes. Crystallization was carried out at temperatures in the region of the main DTA exothermic peak determined for each glass. The glasses were first heated according to the DTA results at the endothermic peak temperature for 5 hrs, which was followed by another thermal treatment at the exothermic peak temperature for 10 hrs.

Identification of crystal phases precipitating due to the course of crystallization was conducted by the X-ray diffraction (XRD) analysis using XSPEX, X-ray diffraction with search/match option, version 5.45, Diano Corporation, Woburn Massachusetts 01801, USA. The crystallization characteristics and internal microstructures of the resultant materials were examined by using scanning electron microscopy (SEM). Representative electron micrographs were obtained using Jeol, JSM-T20 scanning electron microscope.

The coefficients of thermal expansion (α -values) of the investigated samples were carried out on 1.5-2.0 cm long rods using Linseis L76/1250 automatic recording multiplier Dilatometer with a heating rate of 5 °C/min. The linear thermal expansion coefficient was automatically calculated using the general equation:

$$(\alpha) = (\Delta L/L) \cdot (1/\Delta T)$$

where (ΔL) is the increase in length, (ΔT) is the temperature interval over which the sample is heated and (L) is the original length of the specimen.

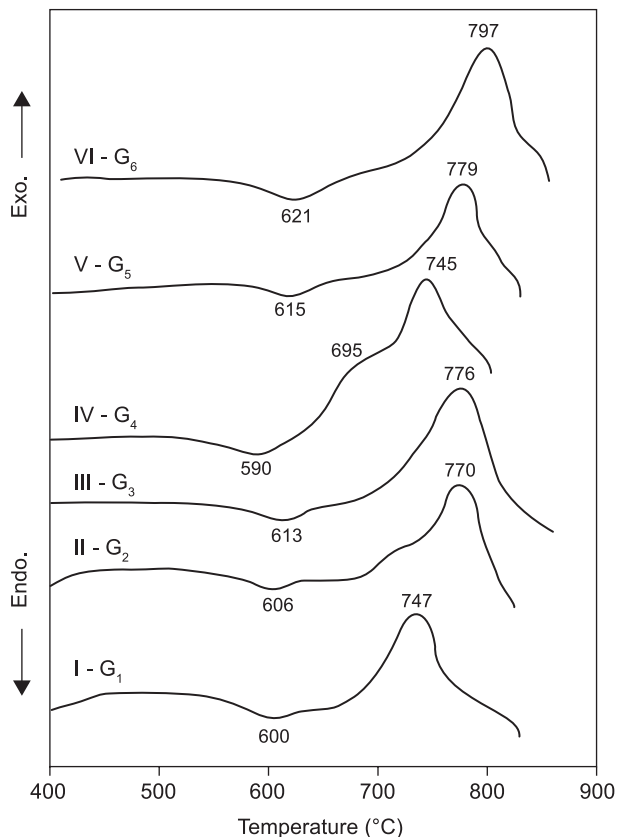


Figure 1. DTA curves of the studied glasses (G_1 - G_6).

RESULTS

Differential thermal analysis

The DTA data (Figures 1-2) of the investigated glasses showed endothermic effects at the 570°-680 °C temperature range. These represent the proceeding phenomena of the glass crystallization. Exothermic effects at the 680°-818 °C temperature range indicated to the crystallization reactions are also recorded.

Crystallization characteristics

The DTA data (Figures 1-2) revealed also that the addition of Al_2O_3 at the expense of Fe_2O_3 in the studied glasses led to shift both the endothermic dips and the onset of the crystallization exothermic peaks to higher temperatures.

The DTA data (Figures 1-2) of the glasses (G_1 - G_{12}) revealed that the addition of $LiInSi_2O_6$ at the expense of $CaMgSi_2O_6$ led to shift the endothermic dips and the onset of the crystallization exothermic peaks to lower temperatures.

The Scanning electron micrographs (Figures 3-6) showed the effect of increasing Al_2O_3 and $LiInSi_2O_6$ contents on the grain microstructure of the materials. SEM micrograph of fractured surface of C_1 clearly showed that volume crystallization of fibrous and

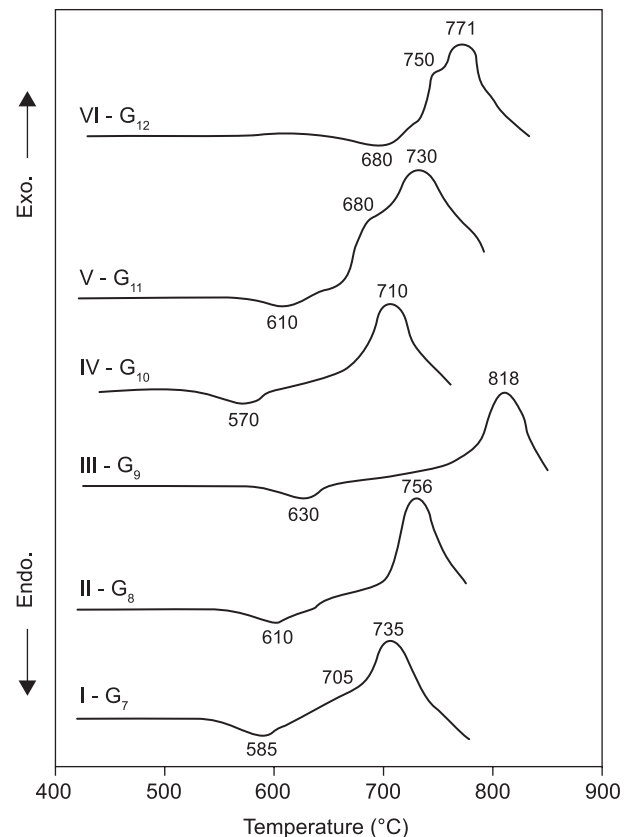


Figure 2. DTA curves of the studied glasses (G_7 - G_{12}).

tiny aggregates-like growths were formed (Figure 3). On increasing Al_2O_3/Fe_2O_3 replacement, i.e. C_3 a well developed rounded like crystals were formed (Figure 4). On increasing $LiInSi_2O_6$ at the expense of $CaMgSi_2O_6$, i.e. C_7 , fine network-like growths were developed (Figure 5). For sample C_{11} (free of $CaMgSi_2O_6$), volume crystallization of tiny aggregate crystals was developed (Figure 6).

The X-ray diffraction analysis (XRD) (Figure 7, Pattern I, Table 2), indicated that the base glass G_1 crystallized at $600\text{ }^\circ\text{C}/5\text{ h} - 745\text{ }^\circ\text{C}/10\text{ h}$ to yield only hedenbergite-magnesian - $Ca(Fe,Mg)(SiO_3)_2$, (Card No. 24-205), α -lithium ferrite - $\alpha\text{-LiFe}_5O_8$ (Card No. 17-115), lithium metasilicate- Li_2SiO_3 (Card No.15-519) and α -quartz (Card No. 5-490) phases.

The addition of 4 mol.% of Al_2O_3 instead of Fe_2O_3 , i.e. G_2 , and heat-treated at $605^\circ\text{C}/5\text{h} - 770^\circ\text{C}/10\text{h}$ led to the development of diopside - $CaMgSi_2O_6$ (Card No. 19-239), lithium aluminium silicate - $Li_{0.6}Al_{0.6}Si_{2.4}O_6$ -

virgilite (Card No. 13.250), α -lithium ferrite - ($\alpha\text{-LiFe}_5O_8$) and lithium metasilicate phases (Figure 7, Pattern II). On increasing Al_2O_3/Fe_2O_3 replacement up to 7.18 mol.%, i.e. G_3 (free of Fe_2O_3) heat-treated at $615^\circ\text{C}/5\text{h} - 775^\circ\text{C}/10\text{h}$, lithium aluminium silicate - $Li_{0.6}Al_{0.6}Si_{2.4}O_6$ phase was developed as a major phase together with diopside and lithium metasilicate phases as indicated from XRD analysis (Figure 7, Pattern III, Table 2).

At low addition of 10 wt% of $LiInSi_2O_6$ at the expense of $CaMgSi_2O_6$, i.e. G_4 , thermally treated at $590^\circ\text{C}/5\text{h} - 745^\circ\text{C}/10\text{h}$, led to the crystallization of hedenbergite-magnesian- $Ca(Fe,Mg)(SiO_3)_2$ as a major phase together with α -lithium ferrite- ($\alpha\text{-LiFe}_5O_8$), $LiInSi_2O_6$ (Card No. 33-799), α -quartz, and lithium metasilicate- Li_2SiO_3 phases (Figure 7, Pattern IV, Table 2). The Al_2O_3/Fe_2O_3 replacement up to 4 mole %, i.e. G_5 , heat-treated at $615^\circ\text{C}/5\text{h} - 780^\circ\text{C}/10\text{h}$ resulted into the formation of hedenbergite-magnesian - $Ca(Fe,Mg)(SiO_3)_2$ (major), lithium aluminium silicate - $Li_{0.6}Al_{0.6}Si_{2.4}O_6$, α -lithium

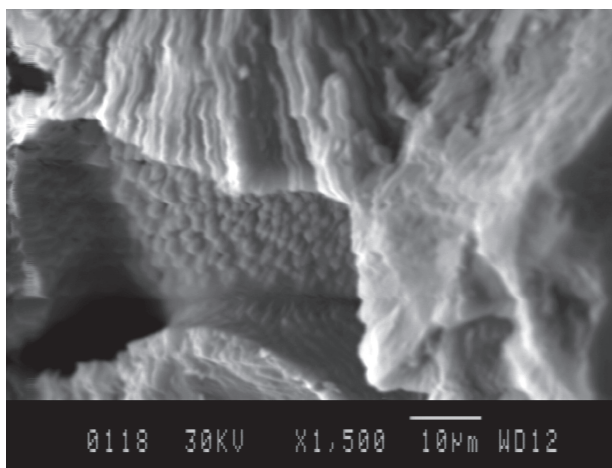


Figure 3. SEM micrograph of fractured surface of glass G_1 crystallized at $600\text{ }^\circ\text{C}/5\text{ h} - 745\text{ }^\circ\text{C}/10\text{ h}$, showed volume crystallization of fibrous - and tiny aggregates - like growths.

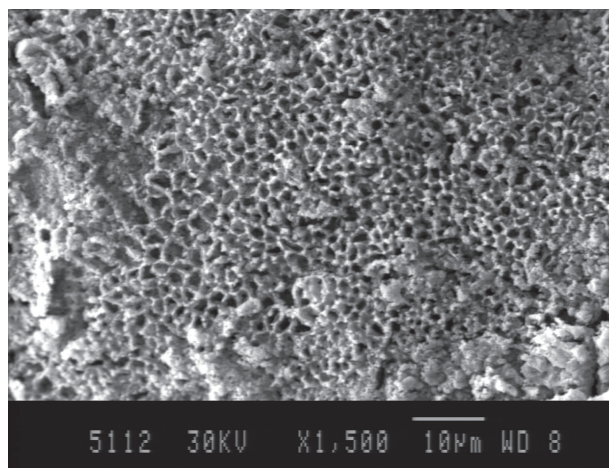


Figure 5. SEM micrograph of fractured surface of glass G_7 crystallized at $585\text{ }^\circ\text{C}/5\text{ h} - 735\text{ }^\circ\text{C}/10\text{ h}$, showed fine network - like growths.

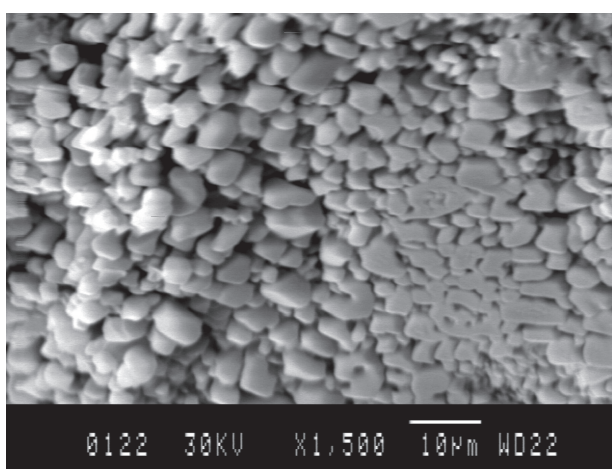


Figure 4. SEM micrograph of fractured surface of glass G_3 crystallized at $615\text{ }^\circ\text{C}/5\text{ h} - 775\text{ }^\circ\text{C}/10\text{ h}$, showed rounded crystals - like growths.

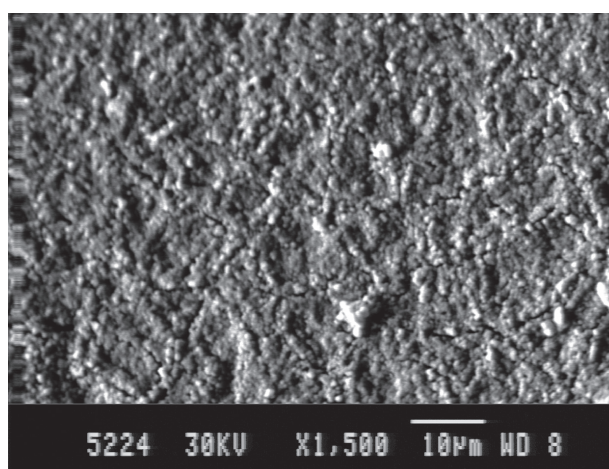


Figure 6. SEM micrograph of fractured surface of glass G_{11} crystallized at $610\text{ }^\circ\text{C}/5\text{ h} - 730\text{ }^\circ\text{C}/10\text{ h}$, showed volume crystallization of tiny aggregate crystals - like growths.

ferrite - α -LiFe₅O₈, LiInSi₂O₆ and lithium metasilicate - Li₂SiO₃ phases as indicated from XRD analysis (Figure 7, Pattern V).

The Al₂O₃/Fe₂O₃ replacement up to 7.44 mol.%, i.e. G₆ (free of Fe₂O₃), heat-treated at 620°C/5h-800°C/10h resulted into the formation of lithium aluminium silicate - Li_{0.6}Al_{0.6}Si_{2.4}O₆ (major), diopside, LiInSi₂O₆ and lithium metasilicate-Li₂SiO₃ phases as indicated from XRD analysis (Figure 7, Pattern VI).

The addition of 30 wt.% of LiInSi₂O₆ at the expense of CaMgSi₂O₆, i.e. G₇, thermally treated at 585°C/5h-735°C/10h, led to the crystallization of hedenbergite-magnesian-Ca(Fe,Mg)(SiO₃)₂ as a major phase together with LiInSi₂O₆, α -LiFe₅O₈ and α -quartz phases as indicated from XRD analysis (Figure 8, Pattern I, Table 2). X-ray diffraction analysis (Figure 8, Pattern II) revealed that the Al₂O₃/Fe₂O₃ replacement up to 4 mol.%, i.e. G₈, heat-treated at 610°C/5h-755°C/10h, led to the formation of hedenbergite-magnesian - Ca(Fe,Mg)(SiO₃)₂ as a major phase together with LiInSi₂O₆ and lithium aluminium silicate - Li_{0.6}Al_{0.6}Si_{2.4}O₆ phases. The Al₂O₃/Fe₂O₃ replacement up to 8.02 mol.%, i.e. G₉ (free of Fe₂O₃), thermally-treated at 630°C/5h-820°C/10h, led to crystallization of Li_{0.6}Al_{0.6}Si_{2.4}O₆ as a major phase together with Ca(Fe,Mg)(SiO₃)₂ and LiInSi₂O₆ phases (Figure 8, Pattern III).

The addition of 50 wt% of LiInSi₂O₆ instead of CaMgSi₂O₆, i.e. G₁₀, thermally treated at 570°C/5h-710°C/10h, led to the crystallization of LiInSi₂O₆ and lithium iron silicate-LiFeSi₂O₆ (Card No. 26-1441) phases as indicated from XRD analysis (Figure 8, Pattern IV, Table 2). The Al₂O₃/Fe₂O₃ replacement up to 4 mol.%, i.e. G₁₁, heat-treated at 610°C/5h-730°C/10h, resulted into the crystallization of β -eucryptite ss as a major phase together with LiInSi₂O₆, indium silicate-In₂Si₂O₇ (Card No. 30-633) and α -LiFe₅O₈ phases (Figure 8, Pattern V). The Al₂O₃/Fe₂O₃ replacement up to 8.71 mol.%, i.e. G₁₂, heat-treated at 680°C/5h-770°C/10h, led to the development of β -eucryptite solid solution as a major phase together with LiInSi₂O₆ phase as indicated from XRD analysis (Figure 8, Pattern VI).

Thermal Expansion

The measurements of the thermal properties, i.e. dilatometric transformation (T_g) and softening (T_s) temperatures as well as the coefficients of thermal expansion (α -values) of the studied glasses and their corresponding glass-ceramic materials were carried out.

Generally, the partial addition of Al₂O₃ instead of Fe₂O₃, decreased the α -values of the studied glasses and also increased both the T_g and T_s values as compared with those free of them (Table 3). The obtained data clearly indicated also that the partial addition of LiInSi₂O₆ at the expense of CaMgSi₂O₆ in the glass, increased the α -values of the glasses, and decreased their transformation (T_g) and softening (T_s) temperatures (Table 3).

For the crystalline material, the Al₂O₃/Fe₂O₃ and LiInSi₂O₆/CaMgSi₂O₆ replacements led to decrease the α -values of the studied glass-ceramics, Table 3. The addition of LiInSi₂O₆ at the expense of CaMgSi₂O₆ led to decrease the α -values of the studied glass-ceramics (e.g. C₄, C₇ and C₁₀).

DISCUSSION

The structure of multicomponent silicate glasses is based on a polymeric network with coexisting cations, which may act as modifiers or as charge compensating cations needed for balancing the charge deficit of oxygen neighbours. This situation occurs when trivalent cations are substituted to silicon in the polymeric network. Glass properties may be strongly affected depending whether cations are network modifiers or charge compensators. This has been shown in alkali-bearing glasses in which transport properties are strongly affected by substitution of silicon by aluminium, in correlation with important structural modifications [10]

It was stated that, in Al₂O₃ containing glasses, the role of Al³⁺ replacing Fe³⁺ is quite different [11]. The ability of aluminum as an intermediate oxide to form the AlO₄ group or to be housed in octahedral coordination

Table 2. Crystalline phases formed in the studied glass-ceramics.

Sample No	Heat-treatment (°C/h)	The Developed phases
G1	600/5-745/10	Ca(Fe,Mg)(SiO ₃) ₂ , α -LiFe ₅ O ₈ , Li ₂ SiO ₃ , α -quartz
G2	605/5-770/10	CaMgSi ₂ O ₆ , Li _{0.6} Al _{0.6} Si _{2.4} O ₆ , α -LiFe ₅ O ₈ , Li ₂ SiO ₃
G3	615/5-775/10	Li _{0.6} Al _{0.6} Si _{2.4} O ₆ , CaMgSi ₂ O ₆ , Li ₂ SiO ₃
G4	590/5-745/10	Ca(Fe,Mg)(SiO ₃) ₂ , α -LiFe ₅ O ₈ , LiInSi ₂ O ₆ , α -quartz, Li ₂ SiO ₃
G5	615/5-780/10	Ca(Fe,Mg)(SiO ₃) ₂ , Li _{0.6} Al _{0.6} Si _{2.4} O ₆ , α -LiFe ₅ O ₈ , LiInSi ₂ O ₆ , Li ₂ SiO ₃
G6	620/5-800/10	Li _{0.6} Al _{0.6} Si _{2.4} O ₆ , CaMgSi ₂ O ₆ , LiInSi ₂ O ₆ , Li ₂ SiO ₃
G7	585/5-735/10	Ca(Fe,Mg)(SiO ₃) ₂ , LiInSi ₂ O ₆ , α -LiFe ₅ O ₈ , α -quartz
G8	610/5-755/10	Ca(Fe,Mg)(SiO ₃) ₂ , LiInSi ₂ O ₆ , Li _{0.6} Al _{0.6} Si _{2.4} O ₆
G9	630/5-820/10	Li _{0.6} Al _{0.6} Si _{2.4} O ₆ , Ca(Fe,Mg)(SiO ₃) ₂ , LiInSi ₂ O ₆
G10	570/5-710/10	LiInSi ₂ O ₆ , LiFeSi ₂ O ₆
G11	610/5-730/10	β -Eucryptite ss, LiInSi ₂ O ₆ , In ₂ Si ₂ O ₇ , α -LiFe ₅ O ₈
G12	680/5-770/10	β -Eucryptite ss, LiInSi ₂ O ₆

in the glass interstices is known [12]. The present results indicated that Al^{3+} preferably exhibited a tetrahedral coordination in the present glass because of the large amounts of oxygen available from the lithia present and this led to increase the connectivity of the glass structure, which explain the shift of endothermic and exothermic peaks towards higher temperature values. It was also stated that [13] alumina “dilute” iron oxides in glasses leading to a more coherent structure.

Salman et al., [14] pointed out that the presence of iron oxide increases the crystallization centers and stimulates the crystallization of the glass during the reheating process giving rise volume crystallization of medium to fine grained textures. Salman and Salama [15] revealed that the state of iron, its coordination and concentration in the glasses mainly determined the nature of the phases formed especially at high Li_2O + Fe_2O_3 content.

Iron oxide can be present in the glass as ferrous (Fe^{2+}) and ferric (Fe^{3+}) ions, and their ratio depends upon the glass composition and melting conditions. In silicate glasses, the ferric cations may occupy octahedral FeO_6 and tetrahedral FeO_4 sites [16], while the ferrous cations occupy only octahedral sites which decrease by increasing the iron content [17]. The presence of appreciable amounts of Li_2O together with Fe_2O_3 in the present glasses, greatly favour the formation of non-bridging oxygen atoms. The high concentration of non-bridging oxygen atoms in silicate glass will favour Fe^{2+} in the network-forming position as Fe^{2+}O_4 . As the number of non-bridging oxygen atoms was greatly increased, the Fe^{2+} ions were oxidized to Fe^{3+} , a large percentage of which would favour network forming position as Fe^{3+}O_4 .

The crystallization process of the glass during the reheating process is known to be connected with the

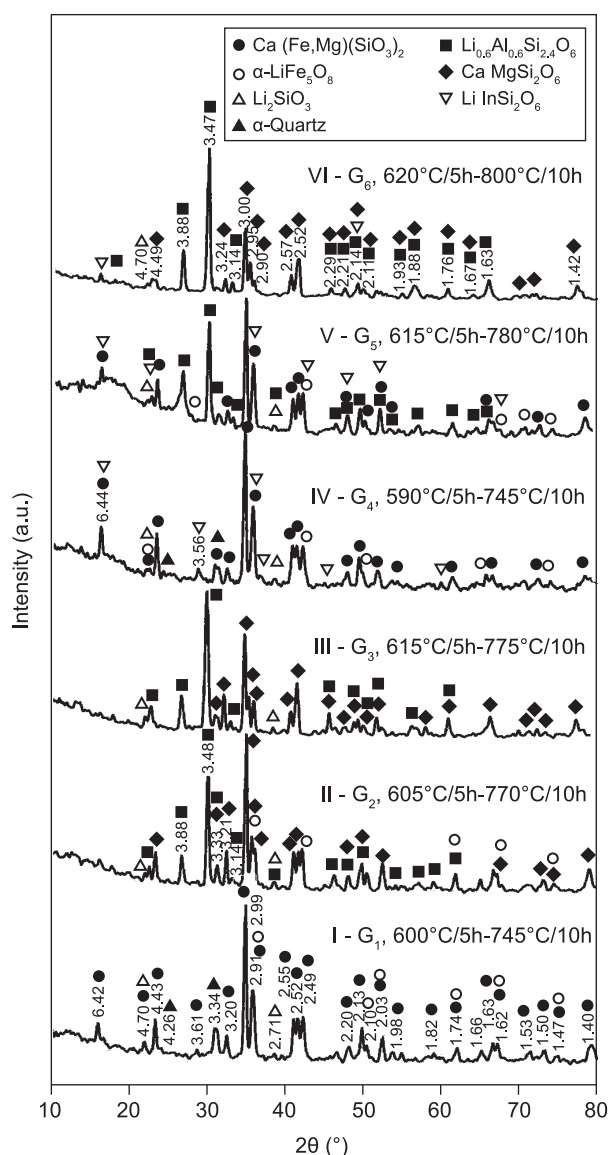


Figure 7. X-ray diffraction patterns of glasses (G_1 - G_6) crystallized at different temperatures.

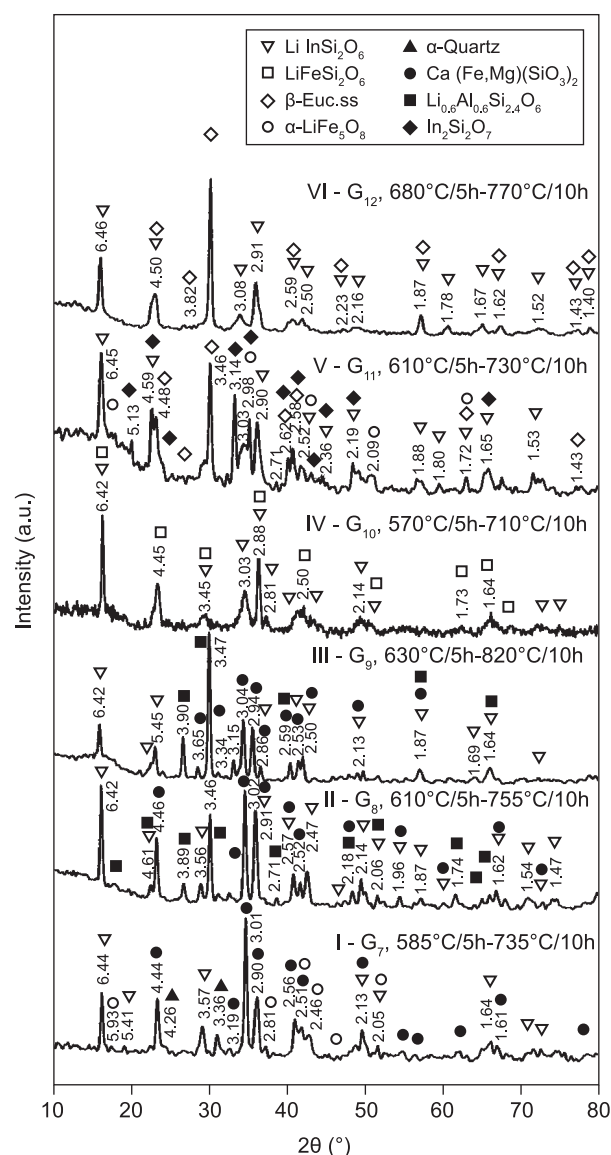


Figure 8. X-ray diffraction patterns of glasses (G_7 - G_{12}) crystallized at different temperatures.

nature and proportions of the glass oxide constituents [18].

The ability of some cations to build glass-forming units or to be housed as modifiers in interstitial positions in the glass structure must also be considered.

The DTA traces revealed also that the addition of $\text{LiInSi}_2\text{O}_6$ at the expense of $\text{CaMgSi}_2\text{O}_6$ led to shift the endothermic dips and the onset of crystallization exotherms of the glasses to lower temperature values. Zou and Hu [19] revealed that the glass transition and crystallization temperatures of these glasses decreased with increasing In_2O_3 content, i.e. low energy is needed to induce crystallization in glasses with higher content of $\text{LiInSi}_2\text{O}_6$.

The present study revealed that the base glass was crystallized to form hedenbergite-magnesian (pyroxene solid solution), α -lithium ferrite, lithium metasilicate and α -quartz phases.

The diopside-hedenbergite minerals form a complete solid solution series between $\text{CaMgSi}_2\text{O}_6$ and $\text{CaFeSi}_2\text{O}_6$. Most of the minerals of this series, however, contain other ions. In general, diopside-hedenbergite minerals of igneous rocks contain some ions replacing Ca, Mg and Fe^{2+} [20]. Hedenbergite is stable below 965°C and when heated at high temperature it inverts to a homogeneous solid solution phase of the same composition.

Pyroxene consists of a group of minerals of variable composition which crystallize fairly readily. They are closely related in crystallographic and other physical properties, as well as in chemical composition [20]. A

wide variety of ionic substitution occurs in the members of the pyroxene group, and there is complete replacement between some of the group components [20], e.g. between diopside ($\text{CaMgSi}_2\text{O}_6$) and hedenbergite minerals from a continuous chemical series with augite and ferroaugite [$(\text{CaMgFe}^{2+})\text{SiO}_3$]. The complexity of this group is exhibited by the wide isomorphism of the various elements in the expandable pyroxene formula [20]:



where $\text{W} = \text{Ca Na}$; $\text{X} = \text{Mg, Fe}^{2+}$, and Mn, Zn, Li ; $\text{Y} = \text{Al, Fe}^{3+}$, Cr, Ti, In , and $p =$ number of ions

The wide range of replacement in the (X, Y) group commonly involving substitution of ions of different charge necessitates compensatory replacement in either the W or Z group, and the replacement must be such that the sum of the charges in the W, X, Y and Z group is 12.

The addition of Al_2O_3 at the expense of Fe_2O_3 led to the formation of diopside instead of hedenbergite-magnesian and lithium aluminium silicate virgilite ($\text{Li}_{0.6}\text{Al}_{0.6}\text{Si}_{2.4}\text{O}_6$) phases. Lithium aluminium silicate virgilite ($\text{Li}_x\text{Al}_x\text{Si}_{3-x}\text{O}_6$) phase has composition corresponds to stuffed disordered β -quartz structure.

The formation of lithium aluminium silicate virgilite ($\text{Li}_{0.6}\text{Al}_{0.6}\text{Si}_{2.4}\text{O}_6$) is enhanced by $\text{Al}_2\text{O}_3/\text{Fe}_2\text{O}_3$ replacements. However, no β -eucryptite or β -spodumene phase could be detected in G_2 - G_9 . This may be attributed to the well known effect of Al_2O_3 in increasing the viscosity of the glass melt and (as compared to Fe_2O_3) [21], a condition which strengthen the structural bond

Table 3. The thermal expansion of the glasses (Gi) and glass-ceramics(Ci).

Sample No.	T_g	T_s	Expansion Coefficients ($10^{-6} \text{ }^\circ\text{C}^{-1}$)						
			α_{25-100}	α_{25-200}	α_{25-300}	α_{25-400}	α_{25-500}	α_{25-600}	α_{25-700}
G ₁	510	538	7.4	7.6	8.0	8.5	–	–	–
C ₁	–	–	8.3	8.3	8.4	8.5	8.5	8.6	8.7
G ₂	522	547	4.9	7.3	7.7	7.3	–	–	–
C ₂	–	–	7.0	7.1	7.2	7.1	7.1	7.2	7.3
G ₃	532	565	4.5	7.0	7.1	7.2	–	–	–
C ₃	–	–	3.4	3.8	4.9	5.0	5.0	5.1	5.1
G ₄	506	534	8.5	8.6	8.8	8.9	–	–	–
C ₄	–	–	8.4	8.4	8.5	8.6	8.7	8.8	8.9
G ₅	514	540	7.0	7.1	7.3	7.5	–	–	–
C ₅	–	–	6.9	7.0	7.1	7.2	7.3	7.4	7.6
G ₆	540	677	6.8	6.9	7.1	7.4	–	–	–
C ₆	–	–	5.8	5.9	6.0	6.1	6.2	6.3	6.4
G ₇	494	522	8.7	8.9	9.0	9.2	–	–	–
C ₇	–	–	7.5	7.8	8.1	8.2	8.3	8.4	8.5
G ₈	514	551	6.8	7.0	7.1	7.3	–	–	–
C ₈	–	–	6.1	6.4	6.4	6.5	6.5	6.6	6.7
G ₉	547	588	6.3	6.8	6.9	7.2	–	–	–
C ₉	–	–	5.0	5.1	5.3	5.4	5.6	5.7	5.8
G ₁₀	483	516	8.9	9.1	9.4	9.7	–	–	–
C ₁₀	–	–	7.0	7.1	7.2	7.3	7.4	7.5	7.5
G ₁₁	513	549	6.3	6.6	6.9	7.1	–	–	–
C ₁₁	–	–	5.0	5.1	5.2	5.2	5.3	5.4	5.5
G ₁₂	567	599	6.0	6.1	6.2	6.5	–	–	–
C ₁₂	–	–	2.1	2.2	2.3	2.4	2.4	2.5	2.5

and reduces the mobility and diffusion of ions in the glass, thus the transformation of virgilite into spodumene becomes difficult.

The present results revealed also that the lithium indium silicate $\text{LiInSi}_2\text{O}_6$ phase was also developed among the crystallization products of the investigated glass-ceramics as a result of adding $\text{LiInSi}_2\text{O}_6$ at the expense of $\text{CaMgSi}_2\text{O}_6$ content in the parent glasses.

The present study revealed also that when Fe_2O_3 and In_2O_3 are present together in lithium silicate glass e.g. G_{10} , the phase distribution can be calculated assuming that Li_2O combines with an equivalent amount of In_2O_3 (or Fe_2O_3) and SiO_2 to form $\text{LiInSi}_2\text{O}_6$ and $\text{LiFeSi}_2\text{O}_6$ pyroxene phases. The $\text{Al}_2\text{O}_3/\text{Fe}_2\text{O}_3$ replacements (i.e. G_{11}) led to the formation of β -eucryptite solid solution, lithium indium silicate, indium silicate and α -lithium ferrite phases and no lithium iron silicate (pyroxene) phase could be detected.

Salman & Mostafa [14] indicated that the α - LiFeO_2 phase was developed in the initial stage of crystallization of iron-containing silicate glass. Salmon & Marcus [22] postulated that LiFeO_2 could form as an intermediate phase during spinel decomposition. Mishra et al. [23] showed that α - LiFeO_2 nucleated and grew in the LiFe_5O_8 matrix and was finally transformed to LiFe_5O_8 spinel phase. In the present glass LiFeO_2 can combine with Fe_2O_3 at 725°C to form LiFe_5O_8 as follows:



The fluctuation observed in the nature of the iron-containing phases formed in the present glasses might be thought to be connected with the state of iron in the glass and change in coordination with its concentration in the glass.

In glass-ceramic G_{12} (free of Fe_2O_3) only β -eucryptite solid solution and lithium indium silicate phases were developed. β -Eucryptite ss is the phase most likely to be formed first even from glasses of stoichiometric spodumene composition, due to the fact that the symmetry of the hexagonal β -eucryptite lattice is closer to the spherically symmetric glass structure than that of the tetragonal β -spodumene [24].

Thermal Expansion

The thermal expansion of the glass is due to anharmonicity of the atomic vibrations. The amplitudes of the thermal vibrations are small when there are many strong bonds present in the network. As a result, the thermal expansion coefficient decreases as the rigidity of the glass network increases. The change in the thermal expansion coefficient of the glass, which is caused by different additives, is often directly proportional to the amounts of the additives [1, 2].

The increase in the thermal expansion of the glass in the transformation range was attributed by Zarzycki [25] to the formation of defects such as vacant anion

sites or incomplete coordination. These defects introduce asymmetries into the short range of glasses and increase the thermal vibration. In the transformation range, glass behaves as a plastic material.

The thermal expansion of glass is not only a function of temperature but also depends, among other factors, on composition. The thermal expansion is also sensitive to the structure of the glass, e.g., degree of polymerization, type of structural units, the nature and contribution of the different cations, whether they occupy forming or modifying positions in the glass network [2].

In the present work, the addition of Al_2O_3 at the expense of Fe_2O_3 content led to decrease the expansion coefficients (α) of the glasses, this is most probably due to the fact that Al^{3+} preferably exhibited a tetrahedral coordination in the present glass because of the large amounts of oxygen available from the lithia present and this led to increase the connectivity of the glass structure, thus the decrease in the α -values of the glasses and the increase in both of the (T_g) and (T_s) values could be expected.

The obtained data clearly indicated also that the partial addition of $\text{LiInSi}_2\text{O}_6$ at the expense of $\text{CaMgSi}_2\text{O}_6$ in the glass, increased the α -values of the glasses, and decreased their transformation (T_g) and softening temperatures (T_s). This could be attributed to the fact that In_2O_3 decrease the connectivity of the glass structure [19] and this led to increase the α -values of the glasses, and decreased their transformation (T_g) and softening (T_s) temperatures.

The thermal expansion coefficient of glass ceramics can differ markedly from that of the glasses. Thermal treatment of the glasses generally introduces crystalline phases having expansion coefficients usually different from that of the parent glass. Therefore, the glass ceramic materials may have high or low coefficients of expansion depending on the crystal phases formed and the residual glass matrix [2].

An extremely wide range of thermal expansion coefficients is covered by the different crystal types and the development of these phases in appropriate proportions forms the basis of the production of glass ceramics with controlled thermal expansion coefficients.

The crystallization of lithium aluminosilicate glasses generally produces crystal phases such as β -eucryptite and/or β -spodumene with much lower expansion coefficients than those of the parent glasses. The contribution of a particular crystal phase to the thermal expansion of a glass-ceramic may be also modified if the crystal enters into solid solution with another phase [25]. Both β -eucryptite and the composition corresponding to $\text{Li}_2\text{O}.\text{Al}_2\text{O}_3.2\text{SiO}_2$ have negative coefficients of expansion. Strnad [26] revealed that, because of its low or even negative thermal expansion coefficient, the stabilization of β -eucryptite ss at room temperature is important for the preparation of low-expansion glass-ceramic materials. β -Eucryptite has high negative ex-

pansion of $-86 \times 10^{-7} \text{ }^\circ\text{C}^{-1}$ ($20^\circ\text{-}700^\circ\text{C}$) and $-64 \times 10^{-7} \text{ }^\circ\text{C}^{-1}$ ($20^\circ\text{-}1000^\circ\text{C}$) [26]. Diopside and hedenbergite which are considered to be pyroxene members have α -values of $(50\text{-}150) \times 10^{-7} \text{ }^\circ\text{C}^{-1}$ ($20\text{-}800^\circ\text{C}$) and 7.2×10^{-7} ($20\text{-}1000^\circ\text{C}$) [26]. It has been reported that lithium disilicate has a-value of $110 \times 10^{-7} \text{ }^\circ\text{C}^{-1}$ ($20\text{-}600^\circ\text{C}$) [26]. α -Quartz has α -value of $237 \times 10^{-7} \text{ }^\circ\text{C}^{-1}$ ($27\text{-}10000^\circ\text{C}$) [26]. While lithium iron silicate-LiFeSi₂O₆ has α -value of $73 \times 10^{-7} \text{ }^\circ\text{C}^{-1}$ ($24^\circ\text{-}800^\circ\text{C}$) [26 & 27]. There is no available data about the expansion coefficients of the LiInSi₂O₆ or In₂Si₂O₇ or a-LiFe₅O₈ phases.

Generally, the Al₂O₃/Fe₂O₃ replacements led to decrease the α -values of the studied glass-ceramics. This could be attributed to the formation of lithium aluminium silicate phases of low expansion coefficients at the expense of the high expanding α -quartz phase.

The experimental data revealed that the glass-ceramic samples containing-LiInSi₂O₆ have low thermal expansion coefficient values. Therefore, the addition of LiInSi₂O₆ at the expense of CaMgSi₂O₆ content led to decrease the α -values of the studied glass-ceramics (e.g. C₄, C₇ and C₁₀). This could be attributed to the development of lithium indium silicate at the expense of high expanding lithium silicate, hedenbergite and α -quartz phases.

According to McMillan [2], in designing glass-ceramics to have specified thermal expansion coefficients, therefore, it is possible to vary not only the types of crystals but also their proportions in order to achieve the desired properties.

CONCLUSIONS

The crystallization characteristics of some glasses based on LiFeSi₂O₆-CaMgSi₂O₆ composition modified with Al₂O₃/Fe₂O₃ and LiInSi₂O₆/CaMgSi₂O₆ replacements was carried out.

The present study revealed that the addition of LiInSi₂O₆ at the expense of CaMgSi₂O₆ led to improve the crystallization tendency of the glasses and decreased the temperature at which the crystallization started.

Varieties of hedenbergite-magnesian, α -lithium ferrite, lithium metasilicate, α -quartz, diopside, Li_{0.6}Al_{0.6}Si_{2.4}O₆, β -eucryptite solid solution, lithium indium silicate, indium silicate and lithium iron silicate phases are mostly detected by the X-ray diffraction analysis.

The crystallization process of the glass during the reheating process is connected with the nature and proportions of the glass oxide constituents.

The partial addition of Al₂O₃ instead of Fe₂O₃, decreased the α -values of the studied glasses and also increased both the (T_g) and (T_s) values. While the partial

addition of LiInSi₂O₆ at the expense of CaMgSi₂O₆ in the glass, increased the α -values of the glasses, and decreased their (T_g) and (T_s) temperatures.

For the glass-ceramics, the Al₂O₃/Fe₂O₃ and LiInSi₂O₆/CaMgSi₂O₆ replacements led to decrease the α -values of the studied glass-ceramics depending on the type and proportions of the crystal phases formed.

References

- Holland W., Beall G.H.: *Glass-ceramic technology*, Am. Ceram. Soc. 2002.
- McMillan P.W.: *Glass-ceramics*, Academic Press, London, N.Y. 1979.
- Petzoldt J., Pannhorst W.: *J. Non-Cryst. Solids* 129, 191 (1991).
- Tulyaganov D.U., Agathopoulos S., Fernandes H.R., Ferreira J.M.F.: *Ceram. Int.* 30, 1024 (2004).
- Salman S.M., Darwish H.: *Ceramics-Silikaty* 50, 88 (2006).
- Karamanov A., Pelino M.: *J. Non-Cryst. Solids* 281, 139 (2001).
- Loser C., Russel C.: *J. Non-Cryst. Solids* 282, 228 (2001).
- Garkova R., Gugov I., Russel C.: *J. Non-Cryst. Solids* 320, 291 (2003).
- Greaves G.N., Ngai K.L.: *Phys. Rev.* 52, 6358 (1995).
- Calas G., Cormier L., Galois L., Jollivet P.: *C.R. Chimie* 5, 831 (2002).
- Williamson J., Tipple A.J., Rogers P.S.: *J. Iron Steel Inst.* 206, 898 (1968).
- Park J.H., Min D.J.: *J. Non-Cryst. Solids* 337, 150 (2004).
- Samia N., Salama S.N., Salman S.M.: *J. Eur. Ceram. Soc.* 1, 61 (1993).
- Salman S.M., Mostafa F.: *Sprechsaal* 118, 622 (1985).
- Salman S.M., Salama S.N.: *Ceram. Int.* 12, 221 (1986).
- Kurkjian C.R., Sigety E.A.: *Phys. Chem. Glasses* 9, 73 (1968).
- Salman S.M.: *Therm. Chim. Acta* 81, 125 (1984).
- Beall H.G., Doman R.C.: *Encyclopedia of Physical Science and Technology* 7, 441 (1992).
- Zou Z., Hu Z.: *J. Non-Cryst. Solids* 201, 246 (1996).
- Deer W.A., Howie R.A., Zussman J.: *Rock forming minerals*, Vol. 2, Longman, London 1963.
- Salmon O.N., Marcus L.: *J. Am. Ceram. Soc.* 43, 549 (1960).
- Mishra R.K., Omer O., Biest V.D., Thomas G.: *J. Am. Ceram. Soc.* 16, 136 (1978).
- Kalinina A.M., Filipovich V.N. in: *The structure of glass*, Vol. 5, p.105, Eds. Toropov N.A., Porai-Koshits E.A., Consultants Bureau, N.Y. 1965.
- Zarzycki J.: *Glass and vitreous state*, Cambridge Univ. Press, N.Y., Port Chester 1991.
- Strnad Z.: *Glass-ceramic materials in glass science and technology*, Elsevier, Amsterdam, 1986.
- Fei Y.: *Mineral Physics and Crystallography, A Handbook of Physical Constants*, Am. Geophysical Union 1995.